A new procedure for calculating the density and energy distribution of localized hopping sites in disordered semiconductors, using low-temperature electrical conductivity data

2008 J. Phys.: Condens. Matter 20 285210

(http://iopscience.iop.org/0953-8984/20/28/285210)

IOP PUBLISHING JOURNAL OF PHYSICS: CONDENSED MATTER

J. Phys.: Condens. Matter **20** (2008) 285210 (8pp) doi:10.1088/0953-8984/20/28/285210

A new procedure for calculating the density and energy distribution of localized hopping sites in disordered semiconductors, using low-temperature electrical conductivity data

J M Marshall[1] **and C Main**[2,3]

[1] Professor Emeritus, University of Wales, Swansea, UK
[2] Division of Electronic Engineering and Physics, University of Dundee, Dundee DD1 4HN, UK

E-mail: c.main@dundee.ac.uk

Received 15 February 2008, in final form 23 May 2008
Published 17 June 2008
Online at stacks.iop.org/JPhysCM/20/285210

Abstract

Quantum mechanical tunneling between localized sites will dominate carrier transport in disordered solids, at sufficiently low temperatures, predicated by the localized state concentration and energy distribution. We previously advanced a simple procedure for interpreting carrier *mobility* data, for an energy-independent density of states (DOS). Here, we show that it can easily be extended to interpret electrical conductivity data, for both energy-independent and energy-dependent DOS distributions. We also show that the concept of transport energy is of considerable value in understanding the factors that underlie the experimental behavior. Furthermore, the new procedure yields credible and entirely self-consistent results when applied to published conductivity data. Finally, we contrast its success with the major inconsistencies that arise when results obtained using the Mott '$T^{-1/4}$' model are examined in more than superficial detail.

1. Introduction

In disordered semiconductors, at sufficiently low temperatures, charge carrier transport becomes dominated by quantum mechanical tunneling ('hopping') between defect states relatively close to the Fermi level. It is then typically found that the activation energy of the electrical conductivity decreases progressively as the temperature falls.

To examine this situation, we have previously [1] employed a very large computer-generated random array of sites to study the carrier hopping *mobility* within it, using Monte Carlo simulation, for the case of an *energy-independent* density of localized states (DOS). We then employed a new procedure to analyze the resulting data, and obtained extremely good agreement with the simulation DOS. Here, we extend the procedure to allow its use with dc electrical conductivity data. We then show, initially using simulation data, that it is very easily implemented, and provides good agreement in respect of both the magnitude and the energy dependence of the DOS. Next, we apply it to data from several prior experimental studies. We show that it eliminates the major discrepancies that emerge when the Mott '$T^{-1/4}$' model [2] is applied. We also show that the concept of a controlling 'transport energy', located appropriately within the localized state distribution, is of considerable value in understanding the factors that actually determine the low-temperature hopping behavior.

2. The Monte Carlo simulation procedure

At temperature T, the rate of carrier jumps from a site of energy E to one at E', over a distance r, is taken to be described

[3] Author to whom any correspondence should be addressed.

via the Miller–Abrahams [3] expression:

$$\nu_j = \nu_0 \exp(-2r/r_0) \begin{cases} \exp(-(E' - E)/kT), \\ \qquad (E' > E) \\ 1, \qquad (E' \leqslant E). \end{cases} \quad (1)$$

Here, ν_0 is the 'attempt to hop' frequency (taken as 10^{12} Hz throughout this study), r_0 is the localization range for the sites, and k is the Boltzmann constant. At finite applied fields, $E' - E$ includes any additional field-induced potential difference between the sites. At low fields, as in our present simulations, the resulting carrier mobility becomes field independent.

As before [1], an array of 960 000 hopping sites, randomly distributed in a volume of $96 \times 100 \times 100$ units was used in the simulations. However, the present studies employed both an energy-independent and an exponentially energy-dependent DOS. The former featured a site density of $N(E) = N(E_F) = 10^{20}$ cm^{-3} eV^{-1}, with the sites having randomly assigned energies in the range $E = E_F \pm 0.25$ eV where E_F is the Fermi energy. This range was chosen to be well in excess of kT at all temperatures investigated, while still avoiding unnecessary dilution of the array by including sites irrelevant to the transport process. The latter had the form $N(E) = N(E_F) \exp((E - E_F)/kT_0)$, with energies measured upwards relative to E_F and with $N(E_F) = 10^{20}$ cm^{-3} eV^{-1} and $T_0 = 500$ K. The site energy range was $0.2 \geqslant (E - E_F) \geqslant -0.1$ eV.

For each site, its Fermi–Dirac occupation probability, $f(E)$, at the temperature under consideration was employed, in conjunction with a random number, in order to select whether or not it was occupied. Sites thus defined as occupied were taken to be unavailable for initial excess carrier generation or for subsequent hopping transitions. For the unoccupied sites, the 16 nearest *unoccupied* neighbors (i.e. those with the highest values of ν_j, using $r_0 = 4 \times 10^{-8}$ cm and an applied electric field of $F = 10^4$ V cm^{-1}) were identified. We separately confirmed that increasing F by an order of magnitude did not alter the resulting calculated mobilities. Periodic boundary conditions were used in the selection, in all three hopping dimensions.

Individual carriers were then initially generated on randomly-selected unoccupied sites, and allowed sufficient simulation time to equilibrate with and to drift within the array. Their resulting net displacements in the field direction were then combined to determine the average drift mobility, μ. The individual steps involved in the Monte Carlo procedure for such simulations are described in more detail, in [4] for example. Finally, the resulting mobility value was used in conjunction with the charge carrier concentration, $n = \int N(E) f(E) \mathrm{d}E$ (easily calculated for the known $N(E)$ distributions), to obtain the electrical conductivity in the form $\sigma = ne\mu$. Before presenting the results in section 4, we will first describe the analytical procedure employed to interpret them.

3. Analytical procedure for the interpretation of electrical conductivity data

From experimental studies, the available parameters are the magnitude, σ, and activation energy, E_σ, of the conductivity at any given temperature T. However, the latter involves both the activation energy of the mobility, E_μ, and the temperature dependence of the carrier concentration, $n(T)$. Therefore, the effect of the latter component must be addressed. Moreover, almost all equilibrated charge carriers can be expected to occupy states closer to the Fermi level than any measured value of E_σ. Thus, only limited information regarding the concentration and energy distribution of these deeper states can be inferred *directly* from the conductivity data, and some form of extrapolation is required.

However, all that we initially require here is the *temperature dependence* of the carrier concentration, rather than its exact magnitude. Now consider two particular cases.

(a) A constant DOS ($N(E_\mu)$) between the energy E_μ and a similar energy below the Fermi level: the integrated carrier concentration over these states, via Fermi–Dirac occupation statistics, is then $n(T) = N(E_\mu)kT \ln(2)$ and thus varies linearly with temperature. Hence, a modified Arrhenius plot of $\ln(\sigma/T)$ versus $1/T$ can be employed to obtain E_μ.

(b) A DOS that decays exponentially from E_μ to E_F and below, with a characteristic temperature T_0: $n(T)$ is then proportional to $((1/kT) - (1/kT_0))^{-1}$. Since we may expect (and will demonstrate for all data below) T_0 to be significantly greater than T in the low-temperature hopping regime, the procedure in (a) can again be employed.

Other forms of $N(E)$ are obviously possible, although perhaps less physically probable. However, having confirmed by inspection that other types of sufficiently weak temperature dependence yield extremely small changes in the calculated parameters, we consider it justified and sufficient to adopt the procedure in (a), hereafter.

Having determined E_μ as above, we now envisage (see section 5 for further discussion) that the rate-limiting transport process for a carrier normally occupying a thermally equilibrated deeper site close to the E_F must involve traversing a typical distance, r_c, and also gaining the necessary energy to access a site close to E_μ.

To identify an appropriate value, r_c can be adjusted until the calculated conductivity is equal to the experimental one. The computation steps for each temperature then comprise:

(i) Calculation of E_μ, as above.
(ii) Choice of an initial seeding value of r_c. Here, one can use $r_c = r_0$, since the final iterated values of r_c are obviously expected to be greater than or equal to this.
(iii) Calculation of the resulting drift mobility, for carriers moving via states close to E_μ, using the conventional expression $\mu = (e\,\nu_0\,r_c^2/6kT) \exp(-2r_c/r_0) \exp(-E_\mu/kT)$.
(iv) Calculation of the volume of a sphere of radius r_c, as $V = 4\pi r_c^3/3$.
(v) Assumption that this sphere must contain *just one* site at an energy close to E_μ (otherwise, a smaller or larger value of r_c would automatically arise). Thus, calculation of the DOS at this energy, as $N(E_\mu) \sim 1/(V\,E_\mu)$.
(vi) Estimation of the carrier density as $n \sim N(E_\mu)kT$ (but see the comment below).

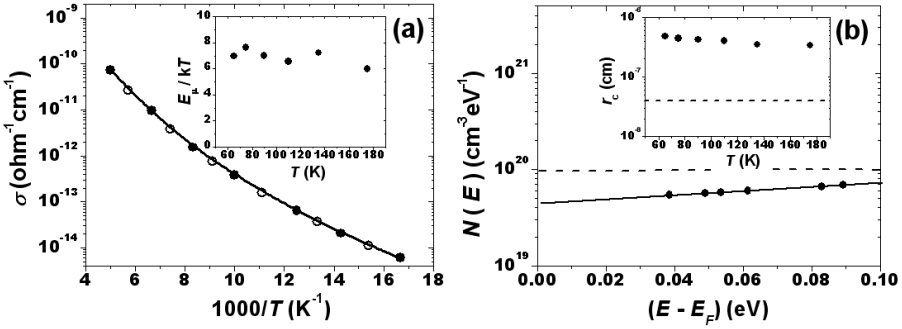

Figure 1. Temperature dependence of the dc electrical conductivity for the energy-independent simulation (a) (filled circles—data points; open circles—fitted σ values) and the DOS calculated using the new procedure (b). The solid line in (a) is a fit as described in the text. That in (b) is an exponential relationship, with a characteristic temperature of $T_0 = 2500$ K, while the dashed line indicates the true DOS. The inset in (a) shows the temperature dependence of E_μ relative to kT. That in (b) is the temperature dependence of r_c, with the dashed line indicating the value of r_0.

(vii) Calculation of the resulting electrical conductivity as $\sigma = ne\mu$.

(viii) Iterative adjustment of r_c, until the calculated conductivity equals the measured one within a specified range (one part in 10^3 hereafter).

Note that step (vi) implicitly assumes that the DOS calculated in step (v) remains constant from the energy E_μ down to and below the Fermi level. Further refinement could be made here (e.g. an initial estimate of the energy variation of the DOS, extrapolated to E_F, could be used in step (vi), in additional iterations). However, here we simply adopt this assumption.

The above steps could be collected into the solution of the equation $\sigma = ar_c^{-1} \exp(-br_c)$. However, we have found that this can give rise to instabilities and/or a lack of convergence. Thus, we below confine ourselves to the use of the above step-wise iterative procedure. This can readily be executed in (e.g.) a very simple computer program, to give extremely rapid convergence in terms of r_c. *An example computer code can be obtained from the corresponding author, upon request.*

4. The simulation data and their interpretation using the analytical procedure

Figure 1(a) shows the temperature dependence of the simulation and calculated dc electrical conductivities, for the energy-independent DOS, and figure 1(b) shows the resulting calculated DOS and r_c parameters. The former includes a fit to a $\ln(\sigma) = A - BT^{-1/n}$ relationship, with the resulting value of n being 8.13. This only significance of this, in terms of the present study, is that it demonstrates that the value of $n = 4$ expected from the Mott '$T^{-1/4}$' model is not obtained. Note, however, that the fitting accuracy is primarily determined by the values of E_μ calculated using adjacent conductivity data points. Thus, although some form of smoothing or curve fitting could be desirable in practice, we have not employed it here.

From figure 1(b), the DOS values calculated via the new procedure are within a factor of 2 of the correct ones (Fermi–Dirac occupation statistics have a negligible effect over this temperature range, as discussed below). They do, however, deviate slightly from the true energy distribution, in yielding a very slowly rising DOS. This is in no respect a consequence of the inclusion of the full Fermi–Dirac statistics in the present study. Essentially identical results were obtained in [1], in which a zero-temperature approximation was employed to specify the number of unoccupied states close to E_F. This is understandable, since the inset in figure 1(a) shows the energies to which the DOS values correspond to be at least $6kT$ above E_F in all cases. These relatively minor discrepancies must thus involve residual deficiencies in the analytical procedure itself. However, we consider that an accuracy of a factor of two or better is highly acceptable, in comparison to many previous attempts to analyze such data (see sections 6 and 7 below, for some examples!).

Figure 2(a) displays the simulated conductivity data for the exponential DOS, and figure 2(b) the calculated DOS values. These are slightly less that the true ones, but again only by a small factor. They yield a value of $T_0 = 416 \pm 5$ K, compared to the actual value of 500 K (i.e. to a rather steeper gradient of the DOS versus energy). Both observations are consistent with those for figures 1(a) and (b). Indeed, assuming an identical influence of the analytical procedure upon the energy dependence of the calculated DOS, T_0' would be $1/(416^{-1} - 2500^{-1}) = 499 \pm 5$ K. Again, the activation energies are much larger than kT, so that Fermi–Dirac occupation statistics do not reduce the density of available hopping sites close to these energies.

It is important to note here that:

(i) The simulation units were normalized to a mean inter-site distance of unity. Thus, if we had selected a different value of $N(E_F)$, then (with the other simulation parameters remaining the same) r_0 would have changed correspondingly. This would leave the subsequent comparison between the calculated and true values of $N(E_F)$ totally unaffected.

(ii) In all of the above computations, the values of r_c remained appreciably higher than r_0 throughout the investigated temperature ranges. Should this criterion cease to be satisfied, the premises of our analytical procedure would

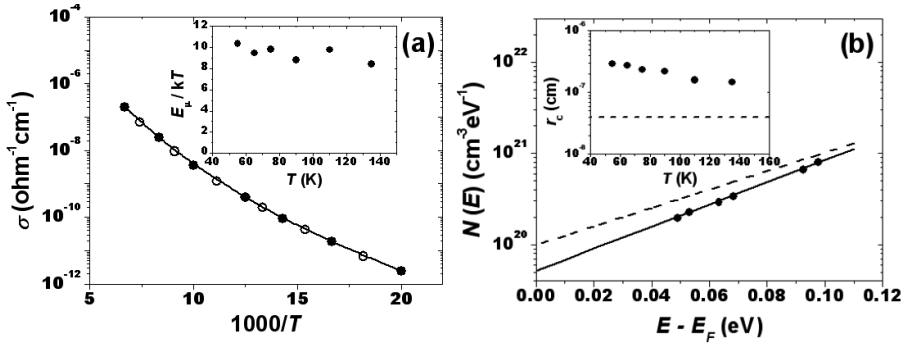

Figure 2. Temperature dependence of the dc electrical conductivity for the energy-dependent simulation (a) (filled circles—data points; open circles—fitted σ values) and the DOS calculated using the new procedure (b). The solid line in (a) is a guide to the eye. That in (b) is a fit of the data to an exponential DOS, with a characteristic temperature of $T_0 = 416$ K, while the dashed line indicates the true DOS. The inset in (a) shows the temperature dependence of E_μ, relative to kT. That in (b) shows the temperature dependence of r_c, with the dashed line indicating the value of r_0.

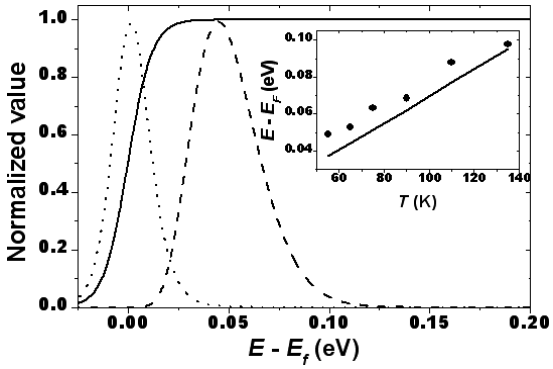

Figure 3. Normalized depiction of the probability of a state being unoccupied, $1 - f(E)$ (solid line), the transport contribution (dashed line) and the equilibrated carrier population (dotted line) for the exponential DOS, at 65 K. The inset shows the calculated transport energies (solid line) with the mobility activation energies (filled circles), at various temperatures.

obviously become invalid. In section 6, we will show that this causes an abrupt rise in the calculated $N(E)$, to physically unrealistic values. We view this as an indication that carrier transport is departing from the low-temperature 'variable range' hopping regime, and becoming dominated by another process such as trap-limited transport via intermittent excitation to and motion within extended states.

5. Relevance of the transport energy concept

For the above data (and for the experimental results below) the conductivity activation energies fall progressively with decreasing temperature. This cannot be due *solely* to an increased hopping distance, since r_c increases only slowly. Moreover, as in figures 1(a) and 2(a) (and below), the mobility activation energies are significantly larger than kT and *increase relative to it* as the temperature falls. We now consider what *does* determine their values.

In this context, it is valuable to introduce the concept of a 'transport energy', E_{tran}. There are various ways in which this can be defined, e.g. [5–8]. However, for our present largely illustrative purposes we do not require a precise quantitative definition. We thus adopt a simplified definition of E_{tran} as that at which the local contribution to the dc conductivity (in terms of the local DOS ($N(E)\mathrm{d}E$), the occupation probability ($f(E)$) and the mobility for transitions to all unoccupied iso-energetic or deeper-lying sites) has a peak value. Despite this simplification, we will demonstrate that the resulting values are in reasonable qualitative agreement with the actual mobility activation energies, as obtained from the simulation data.

Figure 3 shows such a calculation for the simulated exponential DOS, at 65 K. The inset compares the calculated transport energies with the E_μ values. Given the simplistic definition of E_{tran}, we would not expect an exact correspondence. However, the results strongly support an interpretation in which the low-T transport can be viewed in terms of such transport energy—i.e. equilibrated carriers, mostly occupying states within $\sim kT$ of the Fermi level, must access sites close to E_{tran} in order to continue their *macroscopic* motion.

This concept has some similarities to that of trap-limited band transport, (e.g. [9]), but with two very important differences. Firstly, the position of E_{tran} is now temperature-dependent, whereas for trap-limited band transport it is fixed close to the mobility edge. Secondly, the mobility of carriers close to E_{tran} is now much more strongly temperature-dependent. As the temperature falls and E_{tran} moves closer to E_{F}, the total number of iso-energetic or deeper-lying states falls, increasing their average separation and resulting in a reduced mobility.

Note that both the E_{tran} and the E_μ value indicate states sufficiently far above E_{F} that the influence of Fermi–Dirac statistics is minimal. This is also the case for the energy-independent DOS, but is even more so here, where the rising DOS moves E_{tran} to higher energies. The influence of Fermi–Dirac statistics on the total concentration of empty states below E_{tran} (and thus the downwards hopping mobility) is also trivial.

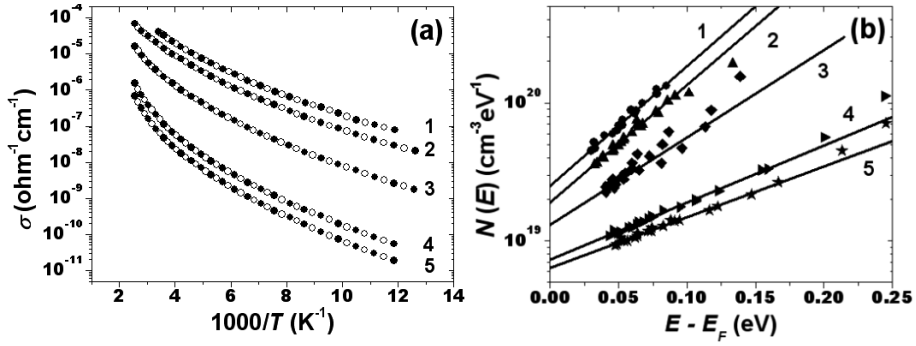

Figure 4. Experimental data (a) (filled circles—data points; open circles—fitted σ values) and the DOS calculated using the new procedure (b), for specimens of r.f. sputtered amorphous silicon [10], as deposited at 300 K and after annealing for 24 h at 383, 523, 653 and 723 K (1 to 5, respectively). The solid lines in (b) employ the fitted values of $N(E_F)$ and T_0.

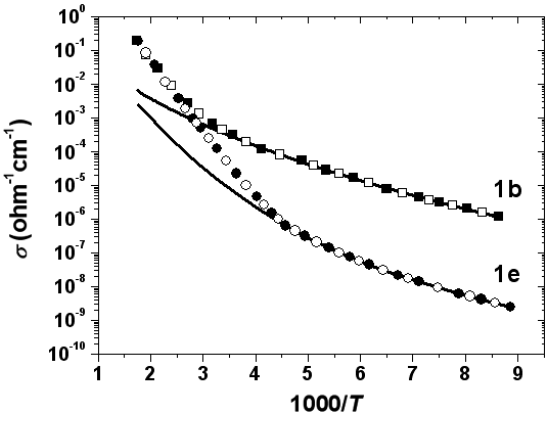

Figure 5. Temperature dependence of the electrical conductivity, for an evaporated specimen of amorphous Ge [11], after two stages of annealing, at 443 (1b) and 583 K (1e). The filled symbols are the experimental data points and the open ones are the fitted values. The lines are fits to the low T data, as explained in the text.

6. Application of the new model to data for amorphous Group IV semiconductors

A meticulously conducted experimental study to which the new analytical procedure can be applied is that of Paul and Mitra [10] for specimens of r.f. sputtered amorphous Group IV (Si, Ge and Ge:Si alloy) films, subjected to various post-deposition annealing treatments. These data are of particular value here, since such early specimens tended to contain much higher densities of defect states close to E_F than have been achieved using subsequent fabrication techniques (and thus featured a much higher contribution due to hopping within such states).

Figure 4(a) shows the published data for a-Si, transferred into an Arrhenius format, for consistency with our previous figures, and figure 4(b) shows the densities of states calculated using our new procedure. Here and below, the assumed underlying parameters were $r_0 = 10^{-7}$ cm and $\nu_0 = 10^{12}$ Hz. Note that physically unreasonable $N(E_F)$ values between 10^{25} and 10^{28} cm^{-3} eV^{-1} were calculated for their various specimens by the original investigators, using a modified version of the Mott model. However, striking anomalies still emerge if the basic $T^{-1/4}$ model, as in [2], is employed. We will return to these in section 7.

Analyses for the a-Ge and a-Ge:Si specimens yielded qualitatively similar results. All appear consistent with exponential energy variations of the DOS, as shown below.

Table 1 summarizes the results, in terms of the calculated values of $N(E_F)$ and the fitted exponential DOS characteristic temperature, T_0. Our present simulation studies suggested that a correction of the form $T_0' \sim 1/(T_0^{-1} - 2500^{-1})$ might be applicable to the T_0 values. This would reduce the energy gradient of the DOS, while having only a small influence on the calculated values of $N(E_F)$. The resulting values of T_0', are therefore also included.

In all cases, higher temperature annealing progressively reduces $N(E_F)$, as seems reasonable. It also yields increased values of T_0 or T_0' (i.e. a reduction in the energy dependence of the DOS), but with differences in detail between the materials.

It is also instructive to compare the above results for a-Ge with those obtained using data presented by Beyer and Stuke [11]. Here, the deposition process was described as one of 'evaporation on a cold substrate with high evaporation rate', but no further details were provided. A single specimen was studied, after successive annealing steps at progressively higher temperatures, for relatively short times (15 min) compared to those in the above study.

Figure 5 shows the temperature dependences of the conductivity, after two of the annealing stages. The fitted lines of the lower temperature data to third order polynomial relationships again have no special physical significance. However, they do assist in indicating the temperatures at which a transition in the transport mechanism seems to occur.

Figure 6 shows the resulting values of the densities of states. In both cases, the low-temperature data correspond well to exponential energy relationships, with $N(E_F) = 1.4 \times 10^{19}$ cm^{-3} eV^{-1} and $T_0 = 320$ K for annealing stage 1b, and $N(E_F) = 6.3 \times 10^{18}$ cm^{-3} eV^{-1} and $T_0 = 630$ K for stage 1e. If the T_0 values are corrected as above, they become approximately 370 and 840 K, respectively. Note that although the authors claimed $T^{-1/4}$ relationships in the low-temperature region, they did not perform calculations of $N(E_F)$ etc. We have done so, and will again indicate the results in section 7.

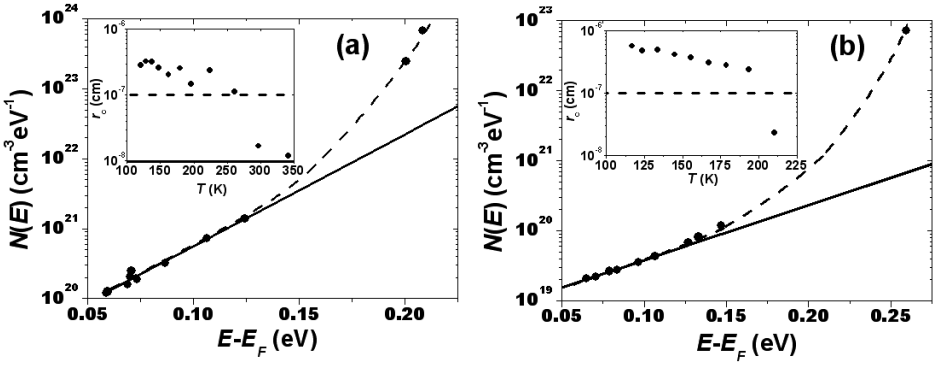

Figure 6. Calculated DOS for the a-Ge specimen in figure 5, after (a) annealing stage 1b and (b) stage 1e. The solid lines in the main figures are fits to an exponential DOS and the dashed lines are guides to the eye. The insets show the corresponding values of r_c. Their dashed lines indicate the value of r_0 assumed in the calculations.

Table 1. Values of $N(E_F)$ (cm^{-3} eV^{-1}) and T_0, for various specimen annealing temperatures and times, as obtained by the analysis of data taken from [10]. The T_0' values indicate the effect of applying empirical corrections to T_0, as described in the text.

a-Si	300 K	383 K 24 h	523 K 24 h	653 K 24 h	723 K 24 h	
$N(E_F)$	2.5×10^{19}	1.9×10^{19}	1.3×10^{19}	7.3×10^{18}	6.4×10^{18}	
T_0 (K)	580	590	795	1220	1370	
T_0' (K)	760	770	1160	2380	3030	
a-Ge	300 K	373 K 1 h	373 K 18 h	473 K 24 h	523 K 24 h	598 K 24 h
$N(E_F)$	7.5×10^{19}	4.9×10^{19}	4.0×10^{19}	2.3×10^{19}	1.9×10^{19}	1.5×10^{19}
T_0 (K)	320	360	370	450	640	640
T_0' (K)	370	420	430	550	860	860
a-Ge:Si	300 K	373 K 2 h	373 K 24 h	473 K 24 h	573 K 24 h	673 K 24 h
$N(E_F)$	3.3×10^{19}	2.6×10^{19}	2.0×10^{19}	1.6×10^{19}	1.2×10^{19}	7.8×10^{18}
T_0 (K)	410	600	610	600	630	750
T_0' (K)	490	790	810	790	840	1070

Given the differences in the annealing conditions, the values of $N(E_F)$ and T_0 are in reasonable agreement with those for the a-Ge specimens in table 1. However, an additional important aspect of figure 6 is the transition between the low-temperature hopping regime, in which our new analytical procedure is applicable, and the higher temperature regime, in which it is not. The calculated values of the parameter r_c in the insets decline (as would be expected) with increasing temperature. However, abrupt falls to physically unreasonable values less than r_0 occur at about 270 and 200 K for cases 1b and 1e, respectively. These temperatures correspond reasonably well to those at which the data in figure 5 deviate from the fitted low-temperature exponential DOS relationships. Although it is not so directly obvious, they also correspond to the activation energy values in figure 6 at which the calculated densities of states deviate from the low-temperature exponential form, and rapidly assume unreasonably high values. All of these features are consistent with a transition to a different conduction mechanism at higher temperatures, such as trap-limited band transport.

7. Evaluation of Mott's '$T^{-1/4}$' procedure, in relation to experimental studies

We previously mentioned that Mott's '$T^{-1/4}$' analytical procedure has often yielded totally unreasonable calculated values of $N(E_F)$. Moreover, as illustrated below, even where the calculated values do not appear unreasonable at first sight, major inconsistencies emerge upon more detailed examination. Despite this, the Mott '$T^{-1/4}$' procedure continues to be employed in an uncritical manner in various studies. The current interest in microcrystalline and nanocrystalline materials has rekindled interest in hopping conductivity, and the model is again being applied uncritically in such cases.

The root cause of the anomalies is that the original version of the Mott model [12] used a parameter, r_{max}, to represent two *very different* quantities—the dominant hopping distance and the radius of a sphere *within which* such hopping occurs. Subsequently [2], a nominal attempt was made to correct this by defining r_{max} as $\int_0^R r^3 r\,dr / \int_0^R r^2\,dr = 75\%$ of the sphere radius, R. This, however, totally neglected the effect of tunneling over varying distances *within* the sphere. The correct expression should be $r_{max} = \int_0^R r^3 \exp(-2r/r_0)\,dr / \int_0^R r^2\,dr$.

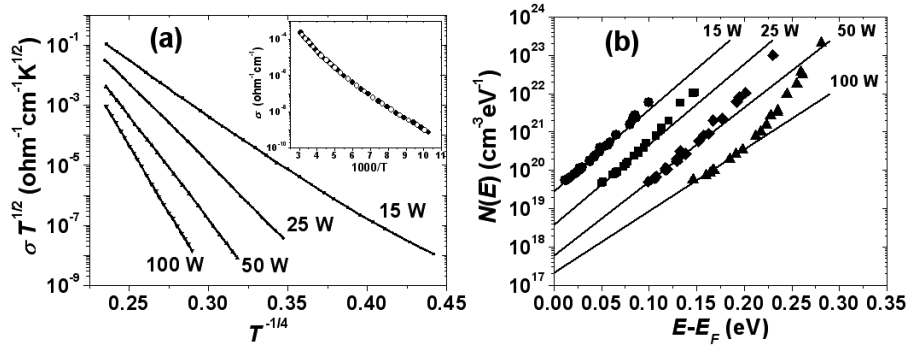

Figure 7. Experimental data (a) and the DOS calculated using our new procedure (b), for sputtered microcrystalline silicon [13], deposited at various r.f. powers. The inset in (a) is an Arrhenius plot of the conductivity, for the specimen deposited at 50 W (the filled circles are the experimental data and the open ones the fitted values). The solid lines in (b) are fits of the lower energy data to exponential relationships, as described in the text.

This only approaches the 75% value for $R/r_0 \ll 1$, which is clearly incompatible with 'variable range hopping'. For $R/r_0 > 3$, $r_{\max}$ falls to less than 1% of the sphere radius!

Further critical inconsistencies arise when the underlying implications of the model are considered in detail. We will illustrate these via a recent study of conduction in microcrystalline silicon films [13]. In doing so, we do not suggest that 'variable range' (i.e. the dominance of transitions beyond nearest neighbor sites) hopping does not occur. Many detailed prior (e.g. percolation-based) studies have predicted this, as do the analyses of our present simulation data. Rather, we wish to emphasize that the attractive simplicity of the Mott model still results in its continued and uncritical use, despite the underlying inconsistencies that would emerge via a proper consideration of the implications.

Of course, it is not obvious that either the Mott model or our present one is appropriate to microcrystalline materials. Here hopping sites will quite probably be concentrated within the grain boundaries around the crystallites, rather than randomly distributed. Therefore, any calculated DOS should be regarded as an 'effective' density of states, as opposed to a true one. Subject to this, it remains worthwhile to demonstrate just how Mott's '$T^{-1/4}$' interpretation yields underlying inconsistencies of such major proportions, in both this and the various other cases above.

Figure 7(a) shows data for sputtered microcrystalline silicon deposited at various r.f. powers. The revised Mott model [2], including the expected temperature dependence of the pre-exponential term, predicts a gradient, for a $\ln(\sigma T^{1/2})$ versus $T^{-1/4}$ plot, of $B = 1.66/(r_0^3 k N(E_F))^{1/4}$. Taking r_0 as 10^{-7} cm as before, the resulting values for $N(E_F)$ are $\sim 3 \times 10^{18}$, 4×10^{17}, 1.5×10^{17} and 5×10^{16} cm^{-3} eV^{-1} for the 15–100 W specimens, respectively. These differ by about a factor of two from those obtained by the original authors, who employed simplified $\ln(\sigma)$ versus $T^{-1/4}$ plots. For our present purposes, we will adopt the values stated herein.

The '$T^{-1/4}$' values of $N(E_F)$ are about an order of magnitude lower than those obtained by the fits in figure 7(b). In itself, this might not be regarded as too dramatic a discrepancy. However, serious problems emerge when we explore the implications in more detail. Below, we illustrate these using the data for the 50W specimen, as shown in the inset in figure 7(a).

Discounting the inappropriate correction to it, the Mott model [2] predicts a hopping distance of $r_{\max} = 3^{1/4}(2\pi N(E_F)kT/r_0)^{1/4} r_{\max} N(E_F)kT/r_0$. At 120 K, this gives a value of 2.4×10^{-6} cm. Note that if a different value of r_0 had been chosen, this would affect $N(E_F)$ in such a way that $r_{\max}/r_0 = 24$ would be unchanged. This also applies to the hopping activation energy $W = 3r_{\max}^3/(4\pi N(E_F)) = 0.123$ eV at 120 K.

Now consider a conventional expression for the resulting carrier mobility:

$$\mu = (e\nu r_{\max}^2/6kT)\exp(-2r_{\max}/r_0)\exp(-W/kT) \quad (2)$$

(as for our procedure in section 3, but with $r_{\max}$ replacing r_c).

With ν as 10^{12} Hz, the pre-exponential term is $\sim$100 cm^2 V^{-1} s^{-1} at 120 K. However, this must be multiplied by a factor of $\sim 10^{-26}$ comprising the combined influence of the two exponential terms, giving an overall mobility of about 10^{-24} cm^2 V^{-1} s^{-1}. With a carrier density $n \sim N(E_F)kT \sim 1.5 \times 10^{15}$ cm^{-3}, this yields an electrical conductivity of $\sigma = ne\mu \sim 2.5 \times 10^{-28}$ Ω^{-1} cm^{-1}. From figure 7(a) (inset), the true conductivity at 120 K is $\sim 10^{-8}$ Ω^{-1} cm^{-1}, giving a discrepancy of almost twenty orders of magnitude. Such inconsistencies do not, *and indeed cannot*, arise for our new procedure. This employs the measured conductivity and its activation energy, to *directly* identify a value of the dominant hopping distance that must automatically then yield full agreement with the measured data (as shown in various figures).

Table 2 shows the results of applying Mott's '$T^{-1/4}$' analytical procedure [2] to other data in this paper. It can again be seen that although the $N(E_F)$ values are not unreasonable at first sight, they lead to discrepancies in the resulting conductivities of at least five orders of magnitude.

Figure 7(b) shows the results of applying our new procedure to data extracted from figure 7(a). For consistency with earlier figures, fits have been included for an exponential energy variation of the DOS at the lowest energies. However, there is obviously no guarantee that such an assumed functional dependence is valid, and the data at the higher deposition

Table 2. Values of Mott's '$T^{-1/4}$' parameter, B, plus the resulting values of $N(E_F)$ (cm^{-3} eV^{-1}) and σ_{calc} (Ω^{-1} cm^{-1}), at the temperatures indicated, for various data as presented above. σ_{true} is the true electrical conductivity at the temperature in question.

	B	$N(E_F)$	T	σ_{calc}	σ_{true}
Energy-independent simulation	107	1.0×10^{19}	80	4.5×10^{-21}	6.5×10^{-14}
Exponential DOS simulation	132	4.6×10^{18}	80	1.1×10^{-25}	3.9×10^{-10}
Ref. [10], Specimen 1	69	3.9×10^{18}	100	1.7×10^{-13}	2.0×10^{-8}
Ref. [10], Specimen 3	76	2.7×10^{18}	100	8.8×10^{-15}	8.5×10^{-10}
Ref. [10], Specimen 5	91	1.3×10^{18}	100	1.8×10^{-17}	7.3×10^{-12}
Ref. [11], Specimen 1b	99	9.2×10^{17}	140	1.2×10^{-17}	4.4×10^{-6}
Ref. [11], Specimen 1e	119	4.4×10^{17}	140	5.5×10^{-21}	1.4×10^{-8}

r.f. powers suggest that the values of $N(E_F)$ may well be underestimated by such a fit, in this case. Data for lower measurement temperatures would be required to explore this possibility.

Finally, we note that the major inconsistencies underlying Mott's '$T^{-1/4}$' model were probably first identified over 35 years ago by Brodsky and Gambino [14], albeit using a rather different approach to that employed here. Unfortunately, and presumably because of the attractive *apparent* simplicity of the model, they appear to have been largely, if not totally, ignored in many subsequent experimental studies.

8. Further studies

Our new analytical procedure can reproduce the density of localized states employed in simulation studies, within a factor of two or better. It can also be applied in a simple manner to experimental data, yielding reasonable and self-consistent values for both the density and energy distribution of such states close to the Fermi level. It does, however, yield a mildly increased energy dependence of the calculated DOS for the two simulation studies. It would be rewarding if this could be eliminated by further refinement.

Finally, additional experimental measurements on un-hydrogenated (i.e. highly disordered) amorphous Group IV semiconductors, over the widest possible temperature range, would be of considerable value in the further evaluation of the new procedure. It is envisaged that these will be performed and reported upon subsequently.

9. Conclusions

A new procedure for the interpretation of the electrical conductivity associated with hopping at low temperatures in disordered semiconductors has been advanced.

Its validity and effectiveness has been demonstrated using data generated via Monte Carlo simulations of hopping within a very large array of hopping sites.

It has also been applied to various published experimental data, for which it yielded entirely credible and self-consistent values of the density of states at the Fermi level, and of the energy distribution of states above this. The results were also fully consistent with the expected effects of different specimen deposition conditions and of subsequent annealing.

In contrast, the Mott '$T^{-1/4}$' model yielded major inconsistencies. Even when these were not directly evident from the estimated $N(E_F)$ values, they became apparent when the resulting associated parameters were used to compare the predicted and experimental values of the electrical conductivity etc.

Acknowledgments

The authors gratefully acknowledge the stimulation provided by the late Professor Vladimir Arkhipov, via his incisive papers concerning hopping and many other topics, and for encouraging our initial approach to the present study. Vladimir will be sadly missed within our scientific community! We also thank Dr Kostadinka Gesheva for her insistence that the deficiencies implicit in the Mott '$T^{-1/4}$' model should be addressed as herein.

References

[1] Marshall J M 2007 *J. Optoelectron. Adv. Mater.* **9** 84
[2] Mott N F and Davis E A 1979 *Electronic Processes in Non-Crystalline Solids* 2nd edn (Oxford: Clarendon)
[3] Miller A and Abrahams E 1960 *Phys. Rev.* **120** 745
[4] Marshall J M and Arkhipov V I 2005 *J. Optoelectron. Adv. Mater.* **7** 43
[5] Monroe D 1985 *Phys. Rev. Lett.* **54** 146
[6] Bässler H 1993 *Phys. Status Solidi* **175** 15
[7] Arkhipov V I, Emelianova E V and Adriaenssens G J 2001 *Phys. Rev.* B **64** 125
[8] Baranovskii S D, Zvyagin I P, Cordes H, Yamasaki S and Thomas P 2002 *Phys. Status Solidi* **230** 281
[9] Marshall J M 1985 *Rep. Prog. Phys.* **46** 1235
[10] Paul D K and Mitra S S 1973 *Phys. Rev. Lett.* **31** 1000
[11] Beyer W and Stuke J 1974 *Proc. 5th Int. Conf. on Amorphous and Liquid Semiconductors* ed J Stuke and W Brenig (London: Taylor and Francis) p 251ff
[12] Mott N F 1969 *Phil. Mag.* **19** 333
[13] Ambrosone G, Coscia U, Cassinese A, Barra M, Restello S, Rigato V and Ferrero S 2007 *Thin Solid Films* **515** 7629
[14] Brodsky M H and Gambino R J 1972 *J. Non-Cryst. Solids* **8–10** 739